

Platinum–acetylide polymer based solar cells: involvement of the triplet state for energy conversion†

Fengqi Guo, Young-Gi Kim, John R. Reynolds* and Kirk S. Schanze*

Received (in Berkeley, CA, USA) 11th November 2005, Accepted 21st February 2006

First published as an Advance Article on the web 21st March 2006

DOI: 10.1039/b516086c

Relatively efficient photovoltaic devices were fabricated using blends of a phosphorescent platinum–acetylide polymer and a fullerene (PCBM); involvement of the triplet excited state of the platinum–acetylide polymer in photoinduced charge transfer is believed to contribute to the device efficiency.

The use of conjugated polymers in organic light emitting and photovoltaic devices (PVDs) has attracted strong recent interest.^{1–4} For example, the poly(phenylene vinylene) derivative MDMO-PPV and poly(3-hexylthiophene) blended with 1-(3-(methoxycarbonyl)propyl)-1-phenyl[6.6]C₆₁ (PCBM) have been used in bulk-heterojunction PVDs to afford relatively high energy conversion efficiency.^{5,6} In order to achieve high efficiency in organic materials based bulk-heterojunction PVDs, several key events must be optimized: (1) light absorption efficiency within the solar spectrum; (2) exciton diffusion to a donor–acceptor interface; (3) photoinduced charge separation; and (4) carrier collection by the electrodes. While each of these events has an influence on PVD efficiency, the efficiency of photoinduced charge separation is key in determining the overall device efficiency.

Following the pioneering work of Weller, who first demonstrated that photoinduced electron transfer (PET) is a key mechanism for fluorescence quenching in donor/acceptor systems,^{7,8} many investigations sought to elucidate the factors that control the efficiency of photoinduced charge separation.⁹ A significant result from this work is that the efficiency for generating long-lived charge separation is substantially higher when the excited state that precedes PET is a spin-triplet state.¹⁰ Fig. 1 shows the mechanism for PET between a triplet donor and an acceptor (³D* and A, respectively). As shown in this figure, in the geminate ion-radical produced by PET, the e[−]/h⁺ pair is

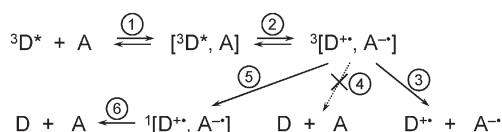


Fig. 1 Mechanism of photoinduced electron transfer. Steps are as follows: (1) diffusion; (2) electron transfer within encounter pair; (3) cage escape; (4) spin-forbidden direct back electron transfer; (5) intersystem crossing in geminate pair; (6) spin-allowed back electron transfer.

Department of Chemistry, Center for Macromolecular Science and Engineering, University of Florida, P. O. Box 117200, Gainesville, FL 32611-7200, USA. E-mail: kschanze@chem.ufl.edu; reynolds@chem.ufl.edu

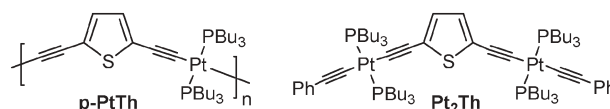
† Electronic supplementary information (ESI) available: Absorption and photoluminescence spectra of *p*-PtTh and Pt₂Th, Stern–Volmer quenching plots. See DOI: 10.1039/b516086c

spin-correlated, retaining its triplet character. Consequently, geminate charge recombination is spin-forbidden, and the probability for the ion-radicals to undergo cage escape is enhanced over that observed in a system in which the excited state preceding PET is a spin-singlet.¹⁰

In a bulk-heterojunction donor–acceptor material, the process of PET at the donor–acceptor interface is the event which produces charge carriers. The process involves PET between a donor–acceptor pair in a low-dielectric, solid matrix. Because of this situation, the Coulomb binding energy in the geminate e[−]/h⁺ pair is substantial,¹¹ and consequently geminate charge recombination is expected to be quite efficient when the pair is a spin-singlet. Consideration of this issue prompted us to ask the following question. Is charge generation efficient in a bulk-heterojunction donor–acceptor material when the excited state that precedes PET is a spin-triplet?

In order to address this question, we designed a bulk-heterojunction material for use in PVDs in which the donor undergoes rapid intersystem crossing to the triplet excited state following photoexcitation. The material we selected uses the platinum–acetylide polymer *p*-PtTh¹² (Scheme 1) as the chromophore and electron donor blended with PCBM as an electron acceptor. The platinum–acetylide was selected because the heavy metal center induces strong spin–orbit coupling, and thus singlet → triplet intersystem crossing is rapid (*k*_{isc} > 10¹¹ s^{−1}) and efficient. In addition, *p*-PtTh is phosphorescent,^{12,13} allowing the use of luminescence quenching to study the interaction between the excited polymer and PCBM. Herein we report that PVDs containing *p*-PtTh/PCBM blends as the active material operate efficiently. Evidence obtained from photophysical measurements suggests that the charge carriers are produced in a PET process involving the triplet excited state of *p*-PtTh.

p-PtTh, model complex Pt₂Th, and PCBM were synthesized as described in the literature.^{13,14} The electronic absorption and emission spectra of *p*-PtTh and model Pt₂Th were measured in *o*-dichlorobenzene (*o*-DCB) solution (see ESI†). The polymer's absorption is dominated by a band at 411 nm, and it exhibits fluorescence and phosphorescence bands with maxima at 436 nm and 608 nm, respectively. The absorption and emission properties of model complex Pt₂Th are very similar to those of the polymer (see ESI†). Importantly, the phosphorescence of Pt₂Th has a



Scheme 1

maximum at 609 nm, indicating that its triplet energy is the same as that of the polymer.

Steady-state and time-resolved emission quenching studies were carried out to probe the interaction between the excited state of *p*-PtTh and PCBM. Addition of low concentrations of PCBM to a solution of *p*-PtTh quenches its phosphorescence. Stern–Volmer plots of the phosphorescence intensity and decay lifetime vs. PCBM concentration are linear (see ESI†), and afford Stern–Volmer quenching constants, $K_{SV} = 6.7 \times 10^4 \text{ M}^{-1}$ (I/I_0) and $4.0 \times 10^4 \text{ M}^{-1}$ (τ_0/τ). The fact that very similar K_{SV} values are obtained for intensity and lifetime quenching indicates that phosphorescence quenching is dominated by diffusional quenching. By using the unquenched lifetime of *p*-PtTh ($\tau_p^0 = 5.8 \mu\text{s}$), the K_{SV} value obtained from the lifetime quenching affords the quenching rate constant, $k_q = 6.8 \times 10^9 \text{ M}^{-1}\text{s}^{-1}$, which is the diffusion-controlled limit in *o*-DCB.

Efficient quenching of the *p*-PtTh phosphorescence by PCBM signals that the latter acts as the acceptor in a process involving either electron or (triplet) energy transfer from the triplet excited state of *p*-PtTh. As outlined in detail below, both electron and energy transfer from $^3p\text{-PtTh}^*$ to PCBM are exothermic. Laser flash photolysis (LFP) experiments were carried out on solutions that contain *p*-PtTh and PCBM in an effort to provide direct evidence for photoinduced electron transfer. Due to strong absorption by PCBM at the laser excitation wavelength (355 nm), it was not possible to obtain definitive evidence for PET as being the dominant quenching mechanism in the *p*-PtTh/PCBM system. However, these experiments show that $^3p\text{-PtTh}^*$ to PCBM energy transfer does not occur.

Due to the greater solubility of Pt₂Th compared to *p*-PtTh it is possible to make concentrated solutions of Pt₂Th to alleviate the problem with competitive absorption by PCBM. In this case LFP provides definitive evidence for PET from $^3\text{Pt}_2\text{Th}^*$ to PCBM. As shown in Fig. 2, at early times following 355 nm excitation the transient absorption is dominated by a band at 610 nm arising

from $^3\text{Pt}_2\text{Th}^*$. At longer delay times the $^3\text{Pt}_2\text{Th}^*$ absorption has decayed, and it is replaced by broad, weak visible absorption and a near-IR band at $\lambda_{\text{max}} \approx 1050 \text{ nm}$. The kinetic traces in Fig. 2 show that the rise of the 1050 nm absorption correlates with the decay of $^3\text{Pt}_2\text{Th}^*$ absorption at 600 nm. The near-IR absorption is clearly due to PCBM^{•−},¹⁵ and it is believed that the visible absorption arises from Pt₂Th^{•+}. The observation of these intermediates combined with the correlation of the rise and decay kinetics provides unequivocal evidence for PET from $^3\text{Pt}_2\text{Th}^*$ to PCBM. It is also important that an absorption at $\approx 700 \text{ nm}$ due to $^3\text{PCBM}^*$ is not observed in the transient absorption spectra;¹⁶ this result shows that $^3\text{Pt}_2\text{Th}^*$ to PCBM energy transfer does not occur.

Photovoltaic devices based on blends of *p*-PtTh and PCBM as the active layer were fabricated on indium tin oxide (ITO) glass substrates that were precoated with PEDOT–PSS (Bayer Baytron-P VP AI4083) as a hole transport layer. The polymer donor and acceptor blend (1 : 4 by wt%) solution was spin-coated onto the PEDOT–PSS layer and the resulting films were dried under vacuum for 2 days at room temperature. Lithium fluoride (0.5 nm) and aluminium (200 nm) layers were sequentially deposited by thermal evaporation on the photoactive layer.

As shown in Fig. 3 and Table 1, *p*-PtTh/PCBM PVDs exhibit a well-behaved photovoltaic effect with an open circuit voltage of 0.6 to 0.7 V and overall efficiency that varies with the thickness of the active layer. *p*-PtTh/PCBM blend films with a thickness of ca. 40 nm were found to afford the best photovoltaic performance under simulated solar illumination with an optical-to-electrical power conversion efficiency of ca. 0.27% (AM 1.5, 100 mW cm^{−2}). As the thickness of the *p*-PtTh/PCBM blend layer is increased from 40 nm to 70 nm, slight drops in the photocurrent density and fill factor were observed. The decrease in photovoltaic performance with increased layer thickness is attributed to an increase in the series resistance of the photoactive layer.

The incident photon-to-current efficiency (IPCE) for a series of PVDs with varied *p*-PtTh/PCBM thickness were measured under low-intensity illumination (Fig. 3). These data are consistent with simulated solar illumination results, *i.e.*, the PV efficiency increases as the thickness of the photoactive layer decreases. The IPCE plots

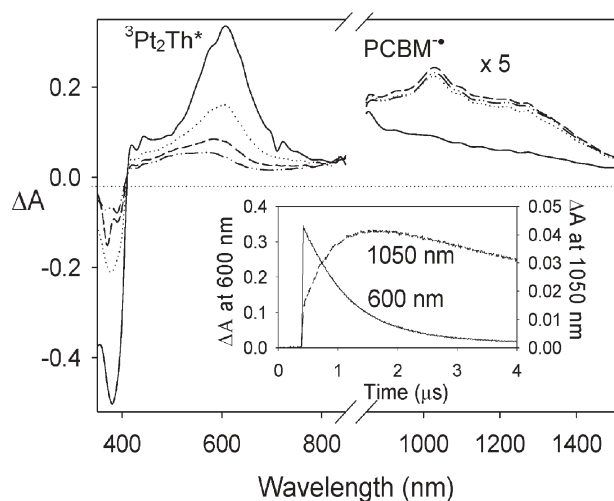


Fig. 2 Transient absorption-difference spectra of Pt₂Th ($c = 0.3 \text{ mM}$) and PCBM ($c = 0.1 \text{ mM}$) in a 1 : 1 mixture of dichloromethane and benzonitrile. Main panel: difference spectra obtained at various delay times following 355 nm excitation (10 mJ per pulse). Delays: (—) 100 ns; (···) 0.64 μs ; (—) 1.28 μs ; (— · —) 1.92 μs . Inset: temporal evolution of transient absorption at 600 nm and 1050 nm.

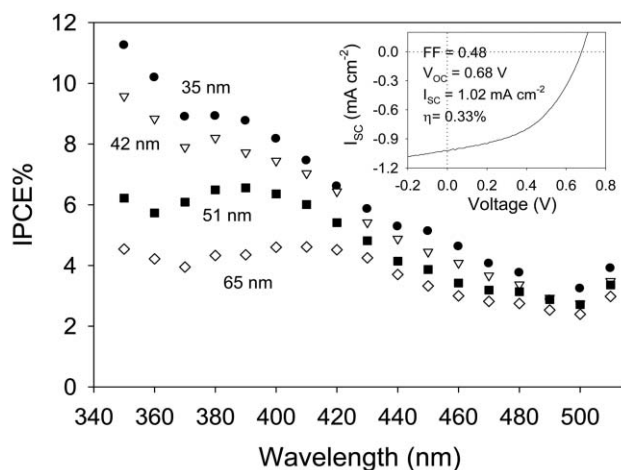
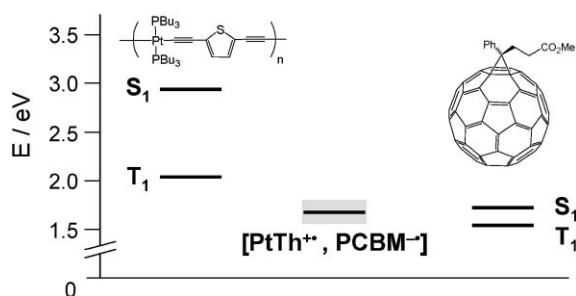


Fig. 3 External quantum efficiency of *p*-PtTh/PCBM solar cells. The composition of the *p*-PtTh/PCBM photoactive layer is 1 : 4 (wt %), and the layer thickness is shown next to plots. Inset: current–voltage characteristic curve under AM 1.5 illumination (100 mW).

Table 1 Summary of I - V characteristics of p -PtTh/PCBM PVDs^{a,b}

η (%)	FF	V_{oc}/V	$I_{sc}/\text{mA cm}^{-2}$	Thickness/nm ^a
0.17	0.4	0.53	0.81	35
0.27	0.43	0.64	0.99	42
0.25	0.39	0.68	0.94	51
0.16	0.34	0.56	0.87	65

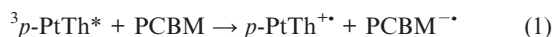
^a Illumination: AM 1.5, 100 mW cm⁻². ^b Photoactive layer is p -PtTh/PCBM (1 : 4 by wt%).

**Fig. 4** Energy level diagram for p -PtTh/PCBM system. Energy levels determined as described in the text.

feature a broad band with a maximum at $\lambda \approx 400$ nm (peak efficiency of ca. 9%) using a 42 nm active layer. The 400 nm band in the ICPE spectra demonstrates that light absorbed by p -PtTh leads to generation of charge carriers. Only 40% of the incident light is absorbed at 400 nm by the 42 nm film; therefore, the internal quantum efficiency for photocurrent in the PVDs is ca. 22%.

The diagram in Fig. 4 provides insight into the mechanism of charge separation in the p -PtTh/PCBM blends. The singlet and triplet energies for p -PtTh are taken from the photoluminescence maxima of the polymer, whereas the corresponding levels for PCBM are estimated by using the values for C₆₀.¹⁵ The energy of the charge separated state, [p -PtTh⁺, PCBM⁻], is estimated from the expression $E_{CS} \approx E_{1/2}(p\text{-PtTh}^{+/0}) - E_{1/2}(\text{PCBM}^{0/-})$,^{9,11} where the oxidation potential of p -PtTh (0.45 V vs. Fc/Fc⁺) was measured, and the reduction potential of PCBM (-1.21 V vs. Fc/Fc⁺) was obtained from the literature.¹⁷ The energy of the charge separated state is estimated to be ca. 1.7 ± 0.1 eV.

Two features are significant with respect to this energy-level diagram. First, the 0.4 eV energy gap between 3p -PtTh* and the charge separated state is sufficiently large so that PET from the polymer triplet state to PCBM is favorable:



The fact that this process is spontaneous and rapid is supported by the LFP experiments on the Pt₂Th/PCBM system in which the products of PET are directly observed. Second, the charge separated state and $^3\text{PCBM}^*$ are very close in energy, and thus PET from p -PtTh to $^3\text{PCBM}^*$ (eqn (2)) is at best only weakly exothermic.



While it is possible that PET could occur as shown in eqn (2), the lack of evidence from the LFP experiments for energy transfer from 3p -PtTh* or $^3\text{Pt}_2\text{Th}^*$ to PCBM makes it unlikely that carrier generation in the p -PtTh/PCBM blends occurs by a mechanism involving energy transfer from 3p -PtTh* to PCBM followed by PET via eqn (2). Since the photoaction spectra clearly show that light absorbed by p -PtTh leads to efficient photovoltaic response, we conclude that charge carriers are produced directly from 3p -PtTh* via eqn (1).

In conclusion, we have demonstrated that blends consisting of a blue-violet absorbing platinum-acetylide polymer with a fullerene derivative can serve as the active material in a photovoltaic device. Photoinduced charge separation in the blends is believed to occur via the triplet excited state of the organometallic polymer. As this is the first report of a polymer-based photovoltaic device in which a triplet excited state is involved in the process of photoinduced charge separation,¹⁸ the relatively efficient response that is observed is significant.

We acknowledge the Air Force Office of Scientific Research (Grant No. F49620-03-1-0091) and the Army Research Laboratory (Grant No. W911NF-04-200023) for support of this work.

Notes and references

- N. S. Sariciftci, D. Braun, C. Zhang, V. I. Srdanov, A. J. Heeger, G. Stucky and F. Wudl, *Appl. Phys. Lett.*, 1993, **62**, 585.
- G. Yu, J. Gao, J. C. Hummelen, F. Wudl and A. J. Heeger, *Science*, 1995, **270**, 1789.
- G. Dennler and N. S. Sariciftci, *Proc. IEEE*, 2005, **93**, 1429.
- S. E. Shaheen, D. S. Ginley and G. E. Jabbour, *MRS Bull.*, 2005, **30**, 10.
- S. E. Shaheen, C. J. Brabec, N. S. Sariciftci, F. Padinger, T. Fromherz and J. C. Hummelen, *Appl. Phys. Lett.*, 2001, **78**, 841.
- P. Schilinsky, C. Waldauf and C. J. Brabec, *Appl. Phys. Lett.*, 2002, **81**, 3885.
- H. Knibbe, D. Rehm and A. Weller, *Ber. Bun. Physik. Chem.*, 1968, **72**, 257.
- D. Rehm and A. Weller, *Ber. Bun. Physik. Chem.*, 1969, **73**, 834.
- Photoinduced Electron Transfer*, ed. M. A. Fox and M. Chanon, Elsevier Science Publishers, Amsterdam, 1989.
- M. Gouterman and D. Holten, *Photochem. Photobiol.*, 1977, **25**, 85.
- H. Oevering, M. N. Paddon-Row, M. Heppener, A. M. Olinger, E. Cotsaris, J. W. Verhoeven and N. S. Hush, *J. Am. Chem. Soc.*, 1987, **109**, 3258.
- N. Chawdhury, A. Kohler, R. H. Friend, M. Younus, N. J. Long, P. R. Raithby and J. Lewis, *Macromolecules*, 1998, **31**, 722.
- K. S. Schanze, E. E. Silverman and X. Zhao, *J. Phys. Chem. B*, 2005, **109**, 18451.
- J. C. Hummelen, B. W. Knight, F. LePeq, F. Wudl, J. Yao and C. L. Wilkins, *J. Org. Chem.*, 1995, **60**, 532.
- J. W. Arbogast, C. S. Foote and M. Kao, *J. Am. Chem. Soc.*, 1992, **114**, 2277.
- K. Matsumoto, M. Fujitsuka, T. Sato, S. Onodera and O. Ito, *J. Phys. Chem. B*, 2000, **104**, 11632.
- M. Keshavarz-K, B. Knight, R. C. Haddon and F. Wudl, *Tetrahedron*, 1996, **52**, 5149.
- While this paper was under revision a manuscript was published describing the use of a phosphorescent small molecule as the donor in PVDs, see: Y. Shao and Y. Yang, *Adv. Mater.*, 2005, **17**, 2841.